Renewable and Sustainable Energy Reviews 26 (2013) 464–479

Contents lists available at ScienceDirect

Renewable and Sustainable Energy Reviews

journal homepage: www.elsevier.com/locate/rser

Research and applications of liquid-to-air membrane energy exchangers in building HVAC systems at University of Saskatchewan: A review

Gaoming Ge*, Mohamed R.H. Abdel-Salam, Robert W. Besant, Carey J. Simonson

Department of Mechanical Engineering, University of Saskatchewan, 57 Campus Drive, Saskatoon, SK, Canada S7N 5A9

ARTICLE INFO

Article history:
Received 26 October 2012
Received in revised form
6 April 2013
Accepted 20 April 2013
Available online 4 July 2013

Keywords:
Semi-permeable membrane
Liquid desiccant
Liquid-to-air membrane energy exchanger (LAMEE)
Run-around membrane energy exchanger (RAMEE)
Energy recovery
Air dehumidification

ABSTRACT

Energy recovery from exhaust air to condition or partly condition outdoor ventilation air has been proved to be an effective method for building energy conservation and is now required in many building Codes and ASHRAE Standards for most commercial buildings. Nonetheless, existing energy recovery ventilators encounter some challenges in practical applications, such as: low exchanger effectiveness and system COP, requirement of adjacent air streams for most exchangers, elimination of cross-contamination between supply and exhaust air, and the avoidance of downstream airborne drift of liquid exchanger coupling fluids. A new kind of liquid-to-air membrane energy exchanger (LAMEE) has been under development in the Thermal Science Laboratory at the University of Saskatchewan, and progress has been made on the research and applications of LAMEEs in heating, ventilation and air-conditioning (HVAC) systems in the past 10 years. The present paper gives a summary of this research. Specifically, properties and selections of semi-permeable membranes and desiccant solutions were studied. Design, steady-state and transient performance of single LAMEEs were investigated. Much attention has also been paid to energy and economic performance of run-around membrane energy exchanger (RAMEE) systems (typically consisting of two LAMEEs) for passive energy recovery in building HVAC systems. Related control and optimization methods for RAMEEs have been developed for some configurations. The application of LAMEEs in liquid desiccant air-conditioning systems as active dehumidifiers and regenerators has been studied.

Contents

* Corresponding author. Tel.: +1 306 966 5476; fax: +1 306 966 5427.
E-mail addresses: gag827@mail.usask.ca, gegaoming@gmail.com (G. Ge).

1364-0321/$ - see front matter © 2013 Elsevier Ltd. All rights reserved.
http://dx.doi.org/10.1016/j.rser.2013.04.022

1. Introduction

Due to population growth and economic development, the annual world primary energy consumption increased, from 7400 million tonnes oil equivalent in 1986 to 12,200 in 2011 [1]. Residential and commercial buildings consumed around 41% of the total primary energy in 2010 [2] and up to 50% of it was accounted by heating, ventilation and air-conditioning (HVAC) systems [3]. Energy conservation of building HVAC systems is one of the most cost-effective ways to reduce the total energy consumption.

Energy recovery from exhaust air and transferring this energy to condition the outdoor ventilation air has been one of the best means to reduce energy consumption and reduce capacity/size of cooling/heating source and air handling equipment in building HVAC systems [4]. Extensive research has been conducted for different types of energy recovery ventilators (ERVs), e.g. energy wheels [5–7], permeable membrane plate exchangers [8–10], twin-tower enthalpy recovery loops [11]. ERVs can precondition the outdoor ventilation air by transferring both heat and moisture between exhaust air and outdoor ventilation air. Up to 60% of annual energy consumption of the HVAC system can be saved depending on the climate and building type, and HVAC system. Nevertheless, the currently available ERVs encounter some challenges for certain applications, such as the requirement of adjacent supply and exhaust air streams, the possibility of cross-contamination between supply and exhaust air, and the desiccant solution downstream drift of liquid desiccant droplets in the supply and exhaust air streams, etc. New energy recovery ventilators that can resolve or mitigate these problems are needed.

Liquid desiccant dehumidification in HVAC systems has been developed because it can avoid energy penalties caused by the overcooling supply air and then reheating it after the water content of the air has been removed by a conventional cooling coil. As well, bacteria growth in stagnate warm water, which may occur in conventional air dehumidification systems, will not occur in desiccant aqueous salt solution coupled systems. Most often, the regeneration temperature of desiccant solution is low so solar energy or waste heat can be more effectively utilized for partially or fully regenerating the salt solution [12,13]. A number of fundamental studies have been carried out on the adiabatic packed-type [14–16] and internally cooled/heated liquid desiccant equipment used as dehumidifiers/regenerators in liquid desiccant air-conditioning (LDAC) systems [17,18]. Several investigations on the performance analysis of LDAC systems have also been conducted in recent years [19–24], where they were more energy-efficient, healthy and environmentally sustainable than conventional vapor compression air-conditioning systems [12,13]. However, for the conventional direct-contact liquid desiccant devices, supply air may cause downstream drift of the desiccant/salt solution and cause corrosion of downstream duct and metal components. Particle downstream drift would impact the indoor environment quality as well. These disadvantages limit the use of the direct-contact liquid desiccant devices in HVAC systems.

The liquid-to-air membrane energy exchanger (LAMEE) is a new liquid desiccant device which uses semi-permeable membranes to transfer heat and moisture. Over the past 10 years, much work has been conducted in the Thermal Science Laboratory at the University of Saskatchewan for the research and applications of LAMEEs in building HVAC systems. This paper gives a review on this research progress. It includes: properties and selections of semi-permeable membranes and liquid desiccants, fundamental research on the heat and mass transfer in LAMEEs, performance of LDAC systems using LAMEEs as active dehumidifiers and regenerators, and energy and economic performance of passive run-around membrane energy exchanger (RAMEE) systems (typically consisting of two LAMEEs) in building HVAC systems.

2. Description of LAMEE and RAMEE

2.1. Constructions of LAMEE and RAMEE

The developed LAMEE is a flat-plate energy exchanger constructed with multiple air and liquid flow channels each separated by a semi-permeable membrane, which is permeable to water vapor but impermeable to liquid water. The semi-permeable membrane allows simultaneous heat and moisture transfer between the air and desiccant solution streams [29]. Fig. 1 shows the construction of a counter-flow liquid-to-air membrane energy exchanger [25].

A RAMEE is comprised of two or more separated liquid-to-air membrane energy exchangers and an aqueous desiccant solution that is pumped in a closed loop between the LAMEEs, as shown in Fig. 2 [26]. In a typical RAMEE system, one LAMEE is installed in the outdoor supply air stream before the air handling unit, and another LAMEE is installed in the exhaust air stream. Heat and moisture are transferred between the air and desiccant solution through the membrane in each LAMEE. Lithium chloride (LiCl), magnesium chloride ($MgCl_2$) or other aqueous salt solutions can be used to transfer energy between the two LAMEEs in a pumped-liquid-coupled-loop (i.e. the RAMEE). Since the volume of desiccant solution changes as it gains or loses water from or to the air streams through the membrane inside each LAMEE, two desiccant reservoirs are placed in the RAMEE system just upstream of each pump.

2.2. Performance evaluation

The most important performance factor of LAMEEs and RAMEEs is the effectiveness (ε). It is the ratio of the actual transfer rate of sensible heat or latent heat or total energy (sensible plus latent) to the maximum possible transfer rate of each type of energy. The sensible effectiveness (ε_{Sen}), latent effectiveness (ε_{Lat}) and total effectiveness (ε_{Tot}) of a single LAMEE can be calculated by Eqs. (1)–(3). These equations assume no energy exchange between the exchanger and its surroundings and $Cr^{*}\geq 1$. Additionally, operating conditions are assumed to be steady-state with no condensation or frosting due to cold LAMEE membrane surface

Nomenclature

A	surface area of membrane (m^2)
C	heat capacity rate (kW/K)
Cr^*	ratio of heat capacity rates (solution/air)
c_p	specific heat capacity(kJ/kg K)
d	channel spacing (m)
H	height of energy exchanger (m) or enthalpy (J/kg)
H^*	operating condition factor
L	length of energy exchanger (m)
m	mass flow rate (kg/s)
NTU	number of heat transfer units
NTU_m	number of mass transfer units
T	temperature (°C)
U	overall heat transfer coefficient (kW/m^2 K)
W	humidity ratio (kg/kg)
X	air properties (temperature, humidity ratio and enthalpy)

Greek letters

ε	effectiveness

Subscripts

air	air flow
exh	exhaust air
in	inlet
Lat	latent
mem	membrane
out	outlet
Sen	sensible
sol	solution flow
sup	supply air
Tot	total
X	sensible, latent or total effectiveness

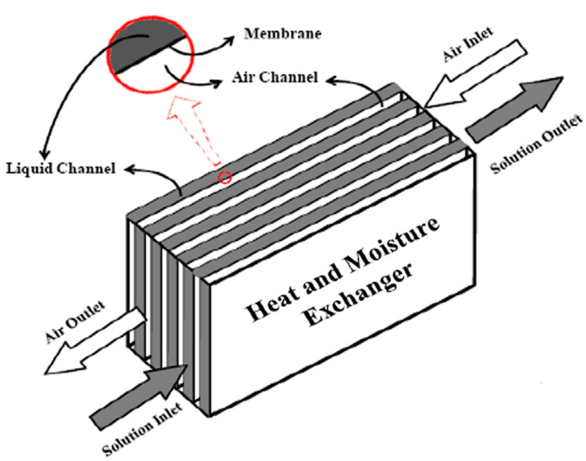


Fig. 1. Construction of a counter-flow liquid-to-air membrane energy exchanger (LAMEE) [25].

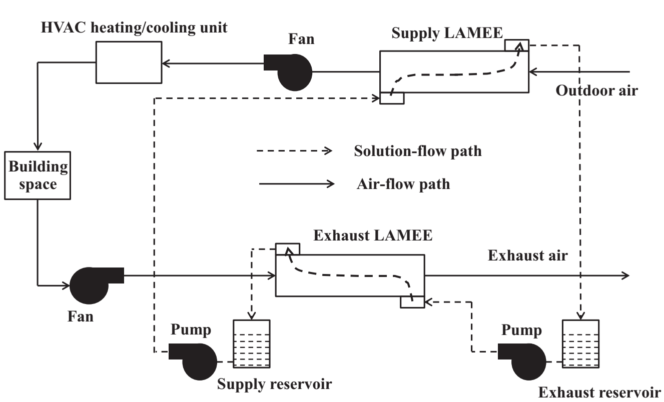


Fig. 2. Schematic of a counter-cross-flow run-around membrane energy exchanger (RAMEE) [26].

temperatures.

$$\varepsilon_{Sen} = \frac{(T_{air,in} - T_{air,out})}{(T_{air,in} - T_{sol,in})} \quad (1)$$

$$\varepsilon_{Lat} = \frac{(W_{air,in} - W_{air,out})}{(W_{air,in} - W_{sol,in})} \quad (2)$$

where $W_{sol,in}$ is the humidity ratio for air in equilibrium with the inlet desiccant solution. Based on the calculated sensible and latent effectiveness, the total effectiveness of the exchanger can be calculated using the following equation [27]:

$$\varepsilon_{Tot} = \frac{\varepsilon_{Sen} + H^* \varepsilon_{Lat}}{1 + H^*} \quad (3)$$

where H^* is the operating condition factor, which is calculated based on air and solution inlet temperatures and humidity ratios in the LAMEE.

$$H^* = \frac{\Delta H_{Lat}}{\Delta H_{Sen}} \approx 2500 \frac{W_{air,in} - W_{sol,in}}{T_{air,in} - T_{sol,in}} \quad (4)$$

For a liquid desiccant coupled RAMEE system with two LAMEEs, the definition of the effectiveness is similar to that for a LAMEE, but the inlet desiccant solution state is replaced by the corresponding inlet state of exhaust air. The effectiveness of the supply and exhaust exchangers are calculated by Eqs. (5) and (6), respectively. The overall effectiveness of the RAMEE is the average value of these two exchangers under steady-state, as shown in Eq. (7).

$$\varepsilon_{X,sup} = \frac{(X_{air,in,sup} - X_{air,out,sup})}{(X_{air,in,sup} - X_{air,in,exh})} \quad (5)$$

$$\varepsilon_{X,exh} = \frac{(X_{air,out,exh} - X_{air,in,exh})}{(X_{air,in,sup} - X_{air,in,exh})} \quad (6)$$

$$\varepsilon_{o,X} = \frac{\varepsilon_{X,sup} + \varepsilon_{X,exh}}{2} \quad (7)$$

where $\varepsilon_{X,sup}$, $\varepsilon_{X,exh}$, and $\varepsilon_{o,X}$ represent sensible, latent or total effectiveness of the supply LAMEE, exhaust LAMEE and the whole RAMEE, respectively. X represents the air temperature, moisture content or enthalpy values.

The heat and mass transfer performance of a single LAMEE or a RAMEE is significantly dependent on two dimensionless parameters. They are the number of heat transfer units (NTU) and the ratio of heat capacity rates between solution flow and air flow (Cr^*), as defined by Eqs. (8) and (9).

$$NTU = Max\left\{\frac{2UA}{C_{air}}, \frac{2UA}{C_{sol}}\right\} \quad (8)$$

$$C_r^* = \frac{C_{sol}}{C_{air}} = \frac{m_{sol} c_{p_{sol}}}{m_{air} c_{p_{air}}} \quad (9)$$

where A is the membrane surface area, C is heat capacity rate, m is mass flow rate, and c_p is specific heat capacity. The subscripts *air* and *sol* represent the air stream and solution flow, respectively.

2.3. Test facility for the LAMEE and RAMEE

A testing apparatus used to test a RAMEE was designed according to ASHARE Standard 84 [28] and it was set up in the Thermal Science Laboratory at the University of Saskatchewan. It consisted of two separate air streams as shown in Fig. 3 [29,30]. One airstream represented the outdoor ventilation air supplied to a building, while the other represented the indoor air exhausted from the building. One LAMEE was installed in each airstream, and both of them were coupled together by a desiccant solution loop to create a complete RAMEE system. The performance of a single LAMEE can also be tested with this facility.

Different supply air temperatures (between −40 °C and 40 °C) and humidity ratios (up to 90% RH) can be provided by an environmental conditioning chamber. The inlet temperature and humidity values of two air streams were kept as close as possible to meet the certification standard test conditions in AHRI standard 1060 (Table 1) [31]. The supply and exhaust air flow rates can be changed by regulating the variable speed fans (3.73 kW each). The flow rate of the desiccant solution can be controlled by using a centrifugal pump capable of flow rate between 0.38 L/min and 5.68 L/min.

In order to evaluate the performance of a RAMEE, it is important to measure the bulk fluid properties of the air streams before and after each LAMEE. The air mass flow rate through each LAMEE was measured using an orifice plate [32] located before and after each exchanger as shown in Fig. 3(a). Temperatures of air streams at the inlet and outlet of each LAMEE were measured by using both T-type thermocouples (average of three thermocouples) and a resistance temperature device (RTD). Humidity was measured at both sides of each LAMEE using capacitive humidity sensors. The temperatures of desiccant solution entering and leaving each LAMEE were measured by T-type thermocouples. A data acquisition system was used to collect and save data from all sensors (i.e., thermocouples, humidity sensors and pressure transducers, etc.) during each test. The central computer can gather 100 data every 10 s at speed of 1 kHz and for each property shows its average using a LabView program.

Table 1
AHRI inlet air conditions for RAMEE performance tests [31].

Summer	$T_{air,in,Sup}$	308.15 K (35 °C)
	$W_{air,in,Sup}$	17.5 g/kg (50% RH)
	$T_{air,in,Exh}$	297.15 K (24 °C)
	$W_{air,in,Exh}$	9.3 g/kg (50% RH)
Winter	$T_{air,in,Sup}$	274.85 K (1.7 °C)
	$W_{air,in,Sup}$	3.5 g/kg (80% RH)
	$T_{air,in,Exh}$	294.15 K (21 °C)
	$W_{air,in,Exh}$	7.1 g/kg (50% RH)

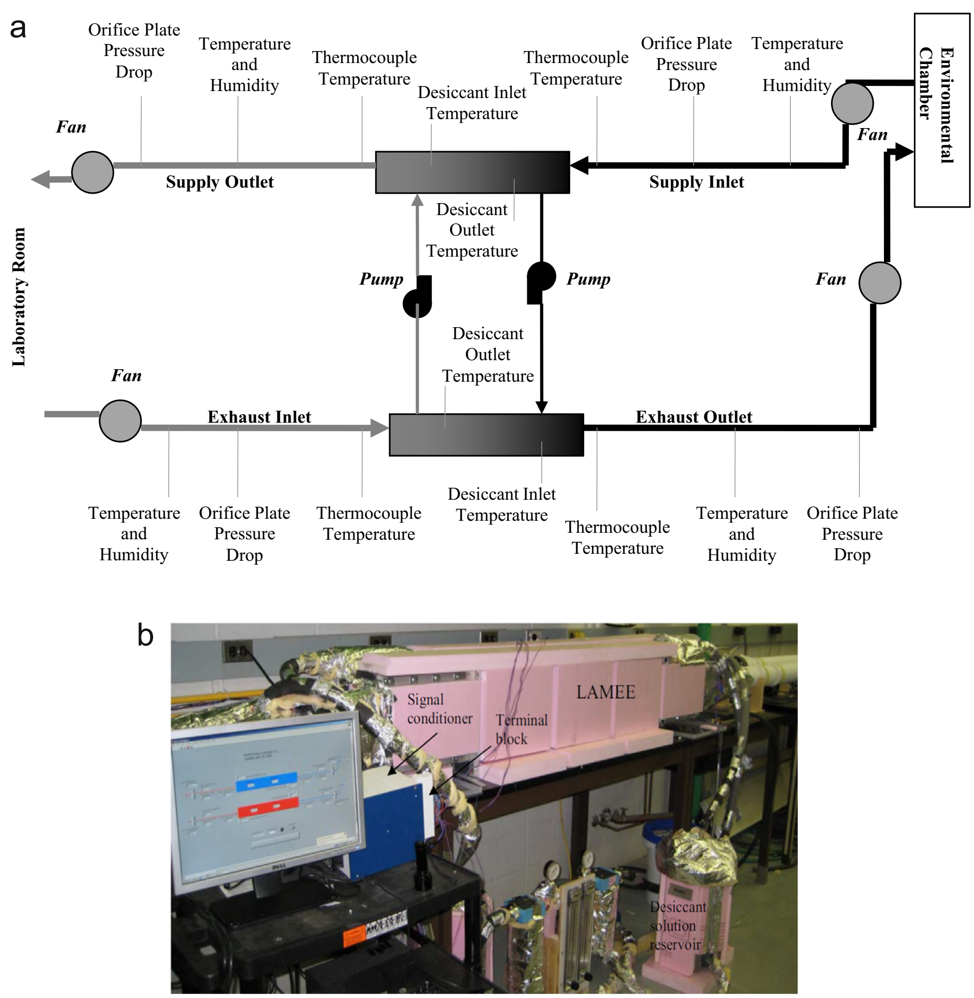


Fig. 3. (a) Schematic [29] and (b) a picture [30] of the RAMEE testing apparatus.

3. Membrane properties and selection

The main difference between the LAMEE and plate heat exchangers is the use of semi-permeable membrane, which can transfer heat and moisture simultaneously. The performance of a LAMEE significantly depends on membrane's properties. The most important membrane properties are vapor diffusion resistance (VDR), liquid penetration pressure (LPP) and modulus of elasticity (*E*) and its linearity.

3.1. Vapor diffusion resistance (VDR)

The vapor diffusion resistance of a membrane used in a LAMEE is critical to the latent and total effectivenesses of the exchanger. The lower VDR, the greater moisture flux for a given moisture content difference. For a given test condition, the latent effectiveness of the LAMEE improves if a membrane with lower VDR is used. The effectiveness of a RAMEE, which mainly consists of two cross-flow LAMEEs, is sensitive to membrane VDR when it is higher than 20 s/m, as shown in Fig. 4 [33].

The vapor diffusion resistance of a membrane can be measured by the Permatran-W® Model 101k test apparatus in our laboratory. In the Permatran-W® test apparatus, the mass flow rate and outlet relative humidity of the high purity nitrogen stream are measured to calculate the water vapor transmission rate through the membrane. In each test, the nitrogen stream passes through a desiccant chamber firstly to ensure that the inlet nitrogen is completely dry. To reduce the precision uncertainty of the test, six simultaneous measurements are taken using six identical test cells, as shown in Fig. 5 [34].

3.2. Liquid penetration pressure (LPP)

The liquid penetration pressure is the water pressure at which liquid water will first pass through a membrane when the liquid pressure is slowly raised. LPP of a membrane should be high enough to prevent the desiccant solution from leaking into the air streams under normal operation. For the tested LAMEEs and RAMEEs in our laboratory, the typical operating pressure was within 34 kPa (5 psi). Hence, the selected membrane should have a LPP higher than this value.

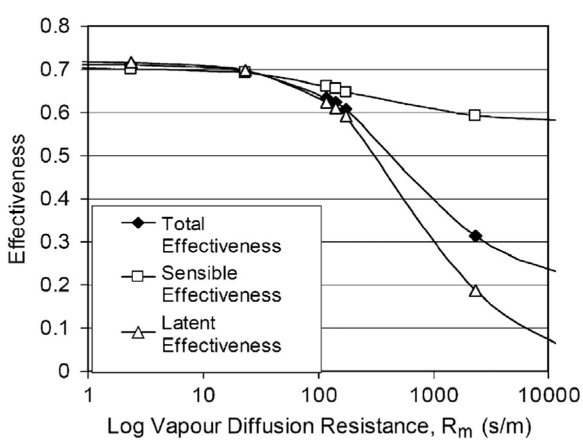


Fig. 4. The dependence of a RAMEE's effectiveness on the membrane VDR [33].

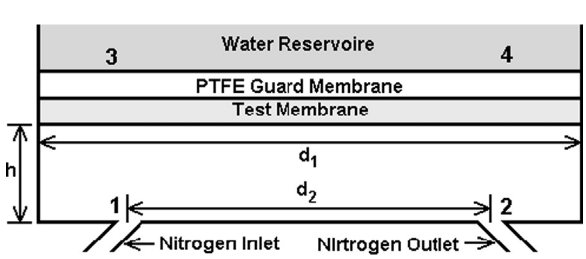


Fig. 5. Schematic of a test cell in Permatran-W® test apparatus [34].

3.3. Modulus of elasticity (*E*)

The membrane elasticity and its linearity over the expected operating range are also critical to the design of LAMEEs or RAMEEs to prevent large membrane deflections. The desiccant liquid pressure in a LAMEE causes the membrane to deflect in the direction of the net force in any unsupported region of the membrane and which is accompanied by strain tangent to the membrane. When this strain is relatively small (i.e., the modulus of elasticity is large and constant over the expected operating range of pressure) one can determine this modulus by an independent test. The lower the membrane modulus of elasticity, the more the membrane will deflect, which will create flow channel variations in the LAMEE. Variations in the LAMEE flow channels can create mal-distributed fluid flows and variations in the mass flow and heat and mass transfer coefficients, which decrease the total effectiveness of RAMEEs. Hemingson et al. [35] found that the total effectiveness of a RAMEE degraded by about 12.5% when the membrane had a peak deflection of 10% of the nominal air channel thickness. Hence, a membrane with higher modulus of elasticity would reduce this reduction in effectiveness.

A liquid penetration and bulge test apparatus has been developed and utilized to test the liquid penetration pressure and modulus of elasticity, as shown in Fig. 6 [36]. For the liquid penetration measurement, the liquid pressure was increased in steps with 0.5 psi intervals every minute. Once three water droplets were observed on the surface of membrane, the pressure was recorded as the liquid penetration pressure. For the modulus of elasticity measurement, the maximum membrane deflection distance for a spherical membrane deformation surface and the liquid pressure can be measured in the same test facility to obtain the membrane stress–strain curve, and consequently compute the membrane modulus of elasticity in the range of a selected test pressure that is normally much lower than the liquid penetration pressure.

3.4. Results of several membranes

There are several available polyethylene and polypropylene semi-permeable membranes which can be employed in the LAMEEs [29]. The properties of various membranes available are presented in Table 2 [33,34]. Considering the properties and their initial cost, the Propore™ and AY Tech. ePTFE Laminate may be reasonable selections due to their small vapor diffusion resistance (VDR), high liquid penetration pressure (LPP), high modulus of elasticity (*E*) and comparatively low cost per unit area. Prototypes with Propore™ [30,37] and AY Tech. ePTFE Laminate [34] and others have been built and tested in our laboratory.

4. Desiccant solution selection

In the LAMEEs and RAMEEs, liquid desiccant solution is utilized as the working fluid to transfer heat and moisture between the air and liquid flows. The liquid desiccant will alter the moisture content of air depending on its temperature and desiccant solution concentration and the adjacent air humidity ratio. If the humidity ratio of the air is greater than the equilibrium humidity ratio of the desiccant solution, the desiccant solution will dry the air. Similarly,

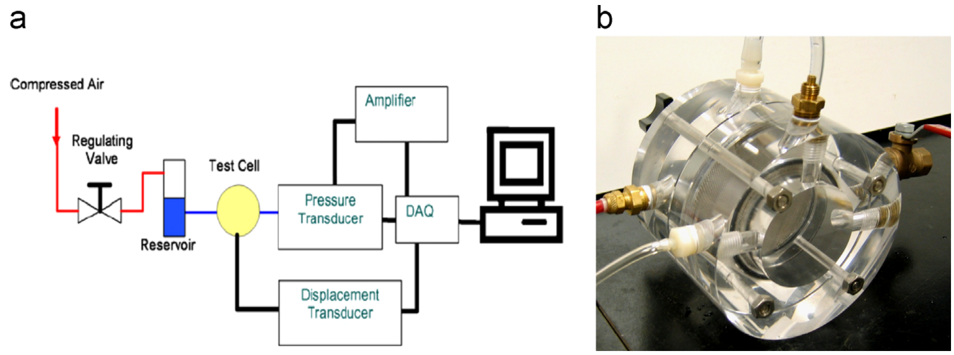


Fig. 6. (a) Schematic of the bulge test facility and (b) a picture of the test cell [36].

Table 2
Summary of properties of various membranes tested [33,34].

	VDR (s/m)	LPP (kPa)	*E* (MPa)	d_{mem} (mm)	Cost ($US/ft^2)
Propore™	158	> 82	17	0.22	$ 0.10
Tredegar #2	5793	> 82	45	0.37	–
Aptra™ RKW	385	> 82	35	0.04	$ 0.35
Porex® PM3V	57	49	12	0.16	$ 40.00
Japanese Tyvek®	329	19	382	0.18	$ 0.15
AY Tech ePTFE Lam	97	> 82	387	0.54	$ 3.27

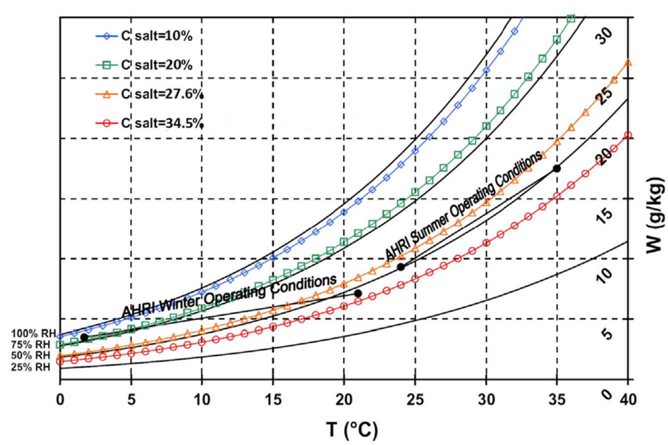


Fig. 7. Equilibrium constant concentration lines of an $MgCl_2$ solution superimposed on the psychrometric chart [38].

if the humidity ratio of the air is lower than the equilibrium humidity ratio of the desiccant solution, the desiccant solution will humidify the air. Fig. 7 shows the constant salt ($MgCl_2$) concentration lines in a psychrometric chart, which indicate the equilibrium conditions for air in contact with an $MgCl_2$ solution at the specified concentrations [38]. The lines of constant concentration are nearly parallel to lines of constant relative humidity.

There are many types of desiccants available and aqueous salt solutions with different salts than $MgCl_2$ will have similar, but shifted, equilibrium salt concentration curves as Fig. 7 and several of these may be suitable for the LAMEE and RAMEE applications [e.g., lithium bromide (LiBr), lithium chloride (LiCl), and calcium chloride ($CaCl_2$)]. All the thermo-physical properties of the desiccant solutions as well as cost should be considered before selecting one of them.

An important consideration for choosing a desiccant is the risk of crystallization within a system and its LAMEEs. It is important that LAMEEs or RAMEEs should operate without any desiccant crystallization because salt crystals attached to the membrane surfaces reduce the moisture transfer between air and desiccant and may cause a flow mal-distribution so the LAMEE's performance will be reduced. In addition, desiccant channel blockage, membrane fouling and improper desiccant pumping are other consequences of the crystallization. According to research conducted by Afshin et al. [39], it was found that under the same operating conditions, crystallization was more likely to occur with $MgCl_2$ followed by $CaCl_2$, LiCl, and LiBr. Also, the air humidity at exchanger inlet was the most significant parameter for the occurrence of crystallization (i.e. the possibility for crystallization increased as the supply or exhaust air humidity decreased). For a cross-flow RAMEE with a total effectiveness of 55% (NTU = 10, and $Cr^* = 3$) operating in a building with indoor air relative humidity (RH) of 50%, crystallization may start when the outdoor humidity was lower than the critical humidity of: 22% RH for $MgCl_2$, 20% RH for $CaCl_2$ and 0% RH for LiCl and LiBr [40]. There was no crystallization risk for LiCl and LiBr in most of the operating conditions. Fig. 8 shows the critical humidity lines for $MgCl_2$ crystallization in a RAMEE used in Phoenix, AZ [39].

Thermo-physical properties of desiccant solutions have an impact on pressure drop in solution channels of LAMEEs. The required pumping power is directly proportional to the pressure drop. Compared to the other three desiccant solutions, $MgCl_2$ has the highest pressure drop value (i.e. $MgCl_2$ solution requires pumping power as much as 2.6 and 3.3 times large compared to LiCl and LiBr solutions). In addition, thermo-physical properties of desiccants solutions affect the desiccant volume changes in different operating conditions. The salt solution volume changes from winter operating conditions to summer conditions, thus, storage tanks are required in order to account for the thermal expansion coefficient of the liquid and the seasonal changes in the liquid salt temperature and concentration. Fig. 9 shows the volume changes of different salt solutions from AHRI summer to winter operation conditions in a tested RAMEE with total 35 L desiccant solution. It is noted that an $MgCl_2$ solution has the smallest variation.

Price is another essential concern for the desiccant solution selection. For a RAMEE prototype (i.e. 35 L of salt solution was required for the RAMEE prototype under AHRI summer equilibrium concentration), Table 3 shows the initial cost, pumping cost, and storage tank size for each of the four liquid desiccants [40]. It can be seen that $MgCl_2$ solution has the lowest initial cost and requires the smallest storage tank, but the operating cost (pumping cost) is highest. The LiCl has a 20 times higher initial cost and requires a 20% larger storage tank than $MgCl_2$.

The impacts of different kinds of desiccant solutions on the effectiveness of energy exchanger were also investigated. Afshin [40] found that the variation in the total effectiveness of a RAMEE operating with various salt solutions as the coupling liquid was very small (i.e. less than 0.5%). Thus the desiccant thermo-physical

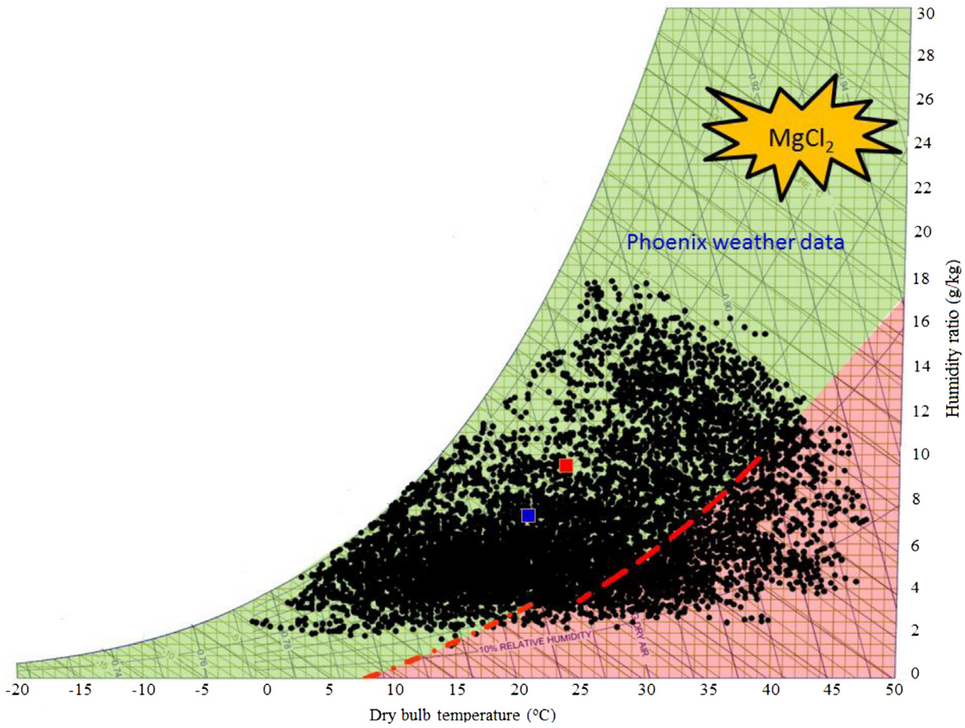


Fig. 8. Hourly climate condition of Phoenix, AZ, superimposed on psychometric chart as well as critical humidity lines for $MgCl_2$ RAMEE with 50% RH indoor conditions [39].

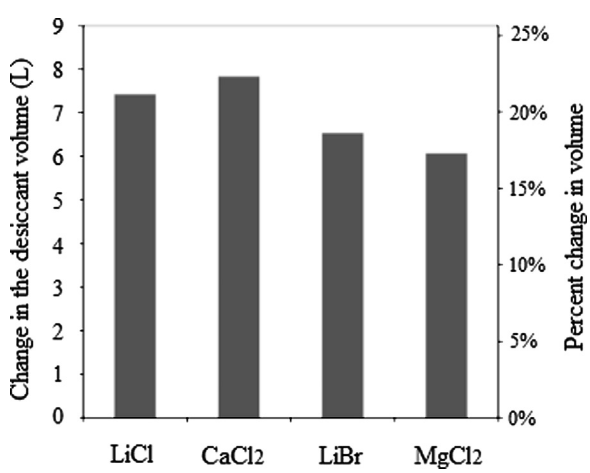


Fig. 9. Volume changes of different salt solutions (35 L) from AHRI summer to winter conditions [40].

Table 3
Relative initial and operating costs and storage tank size of the selected salt solutions in a RAMEE system (all values are relative to the smallest value of one) [40].

Salt solution	Initial cost	Pumping cost	Storage tank size
LiCl	20	1.3	1.2
$CaCl_2$	2	1.9	1.3
LiBr	19	1	1.1
$MgCl_2$	1	3.31	1

properties have a negligible effect on the RAMEE effectiveness provided there is no crystallization.

Although LiBr and LiCl have a very good performance with no risk of crystallization in most climates, their prices are much higher than $MgCl_2$. Using mixtures of different salt solution desiccants may be a promising method to simultaneously reduce the desiccant price and maintain the energy exchanger performance. Mixtures of LiCl and $MgCl_2$ with different mass ratios were tested in our laboratory. The equilibrium humidity ratios of these mixtures were investigated experimentally. It was found that the mixture of LiCl and $MgCl_2$ had an equilibrium relative humidity lower than pure $MgCl_2$ and the mixture's equilibrium relative humidity decreased as the ratio of LiCl increased. For an indoor humidity of 50% RH and temperature of 24 °C, a salt mixture solution with total concentration of 40% with composition of LiCl concentration of 21% and $MgCl_2$ concentration of 19% was found to be safe for use in all North America's cities with very low risk of crystallization when used in a RAMEE, while the price of the mixture was 30% lower than pure LiCl [40].

5. LAMEE design and performance

5.1. Flow configuration

Liquid-to-air membrane energy exchanger can be designed to be counter, cross or counter-cross-flow based on the solution flow configuration relative to the air stream inside the LAMEEs. Fig. 10 shows LAMEEs with different solution flow configurations. The air stream and desiccant solution flow are in opposite directions in the counter-flow LAMEE (Fig. 10(a)) and in perpendicular directions in the cross-flow LAMEE (Fig. 10(b)). In the counter-cross-flow configuration (Fig. 10(c)), the desiccant solution enters and exits through a small portion of the header of the exchanger. At the entrance and exit of the LAMEE, the desiccant solution flows in a cross-flow direction relative to the air; while in the middle of the LAMEE, the solution flows mostly in the counter-flow direction relative to the air flow.

Numerical studies and experimental measurements on the steady-state and transient heat and mass transfer behaviors of the LAMEEs were conducted. The counter-flow exchanger can achieve

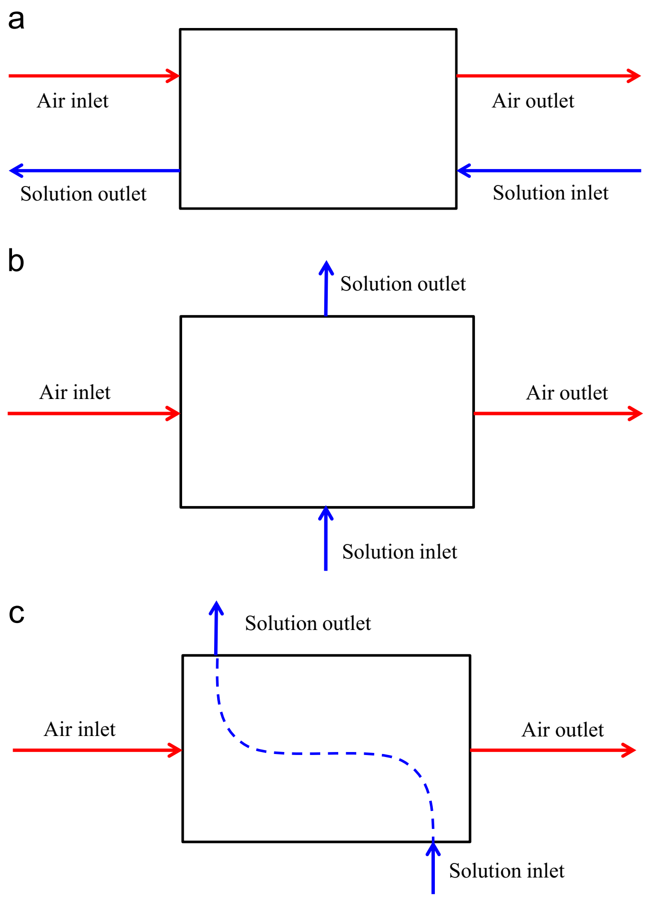


Fig. 10. Air and liquid streams configuration in a (a) counter-flow, (b) cross-flow and (c) counter-cross-flow LAMEE [41].

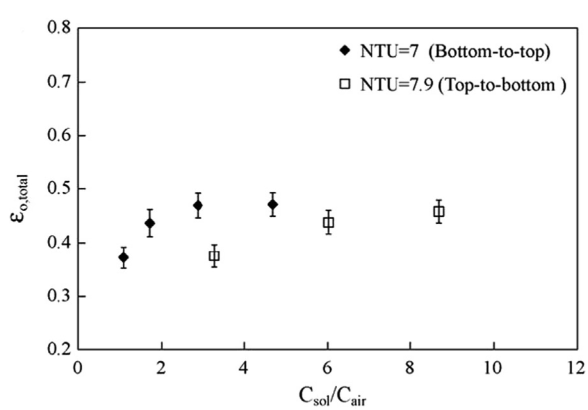


Fig. 11. RAMEE total effectiveness comparison between top-to-bottom and bottom-to-top desiccant solution flow configurations [26].

the highest effectiveness, but this counter-flow configuration is not convenient for manufacturing since the liquid and air flow headers need to be placed side-by-side at the inlet and outlet of the exchanger. The counter-cross-flow configuration can avoid such a problem and its effectiveness can be much better than that of the cross-flow exchanger with the same membrane area. Vali [41] showed that using the counter-cross-flow configuration for exchangers in the RAMEEs typically would increase the effectiveness by approximately 6% compared to RAMEEs with pure cross-flow LAMEEs. Early test results showed that a 55% total effectiveness could be achieved by the counter-cross-flow energy recovery exchanger, which was higher than the minimum total effectiveness (50%) required by ASHRAE Standard 90.1 [42].

In all the three LAMEE configurations, desiccant solution can enter the liquid panels of the exchanger either from the bottom or top. Mahmud et al. [26] found that the top-to-bottom flow configuration in the RAMEE system had lower effectiveness than the bottom-to-top flow configuration, as shown in Fig. 11. In the top-to-bottom flow configuration, the effectiveness was lower because some places inside the liquid panels may not be filled with the desiccant solution or may not have a nearly uniform or homogeneous Cr* or mass flow ratio per unit area. Such a liquid flow mal-distribution would reduce the overall effectiveness. In the bottom-to-top flow configuration, the liquid panels are filled with the desiccant solution and the static pressure distribution is more likely to have similar gradient independent of which flow panel. This type of uniform flow distribution will result in higher effectiveness values. Mal-distribution of the liquid flow is expected to have a smaller effect for bottom-to-top liquid flows, especially when C_{sol}/C_{air} (Cr*) is small. This helps to explain the large difference in effectiveness caused by the flow direction at low Cr* values in Fig. 11.

5.2. Liquid and air channel design

Energy performance and sizing of a LAMEE or RAMEE are dependent on the flow channel spacing, i.e., the solution gap (d_{Sol}) and air flow gap (d_{Air}). Fig. 12 shows that the overall effectiveness of a RAMEE, which consists of two LAMEEs, is less sensitive to the channel size of the liquid flow than to the air channel size [43]. Small air flow and solution flow gaps increase the overall heat and mass transfer coefficient and as a result the size of the exchanger decreases for the same desired total effectiveness. On the other hand, large air and solution flow gaps decrease the overall heat and mass transfer coefficients which result in a bigger exchanger. Therefore, the channel sizes of both the liquid and air flow should be kept at practical small values to achieve a better performance. In the design of a LAMEE or RAMEE, the pressure drops for both air and solution flow channels should be considered as well to ensure low operating costs.

In LAMEE design, air spacer screens have been used to support membranes to prevent excessive membrane deflections because of the

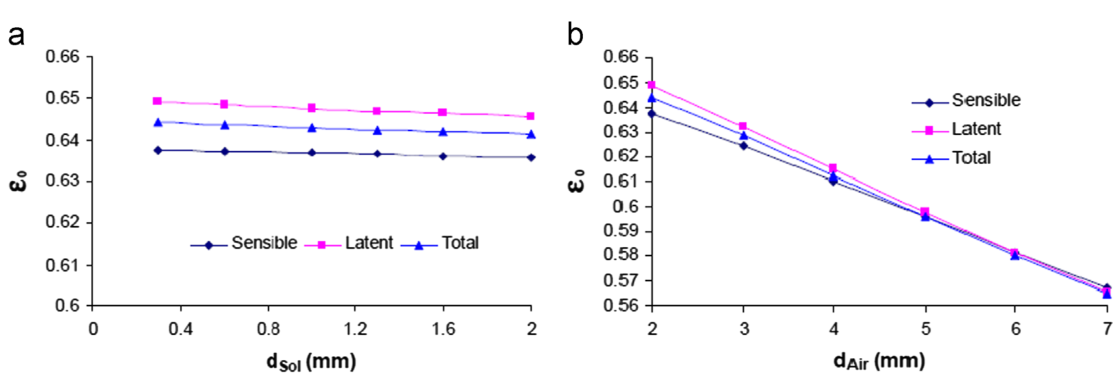


Fig. 12. Overall effectiveness of a cross-flow RAMEE (with two LAMEEs) versus gaps of (a) the liquid channel (d_{Sol}) and (b) the air channel (d_{Air}) [43].

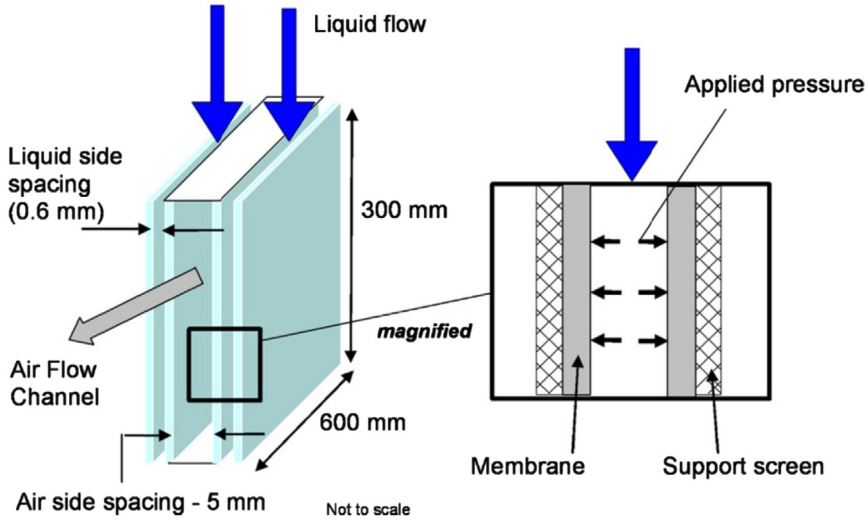


Fig. 13. A schematic of a LAMEE with the support screens [33].

static pressure difference between the liquid flow and air streams. A schematic of a LAMEE with the support screens is shown in Fig. 13 [33]. The air screens inserted in the air channels can play another role. They can enhance the convective heat and mass transfer coefficients in the air side and hence improve the heat and mass transfer rates in the LAMEE. LePoudre [44] numerically investigated the performance of channel flows when sinusoidal porous screen inserts were used. It was found that the thin porous screens could create unstable shear layers in the air flows and enhanced the convective coefficient by up to 87%.

5.3. Steady-state performance

Numerical studies on the temperature and moisture distributions in a cross-flow LAMEE were performed by Fan et al. [43,45,46] and compared with those of a heat exchanger. It was found that the distributions of the isothermal temperature lines in the heat and moisture exchanger were quite different from those in a heat exchanger. The moisture transfer and resulting phase change energy had a great effect on the distribution of the temperature in the exchanger. In the LAMEE, the performance of the exchanger depends on the number of heat transfer units (NTU), the heat capacity ratio (Cr*), and the number of mass transfer units (NTU_m). It was also found that for a given energy exchanger and testing conditions, there was a constant proportional relationship between NTU_m and NTU.

The steady-state performance of a counter-cross-flow LAMEE has been measured by Namvar et al. [47]. The steady-state effectiveness of the LAMEE under different NTU and Cr* was plotted in Fig. 14. The results showed that the effectiveness of a single LAMEE increased generally as NTU and Cr* increased. In addition, the LAMEE was more sensitive to Cr*, especially at lower Cr* values. For instance in Fig. 14(c), with NTU=8 the total effectiveness increased by about 40% when Cr* increased from 1 to 3, but the total effectiveness increased less than 15% when Cr* increased from 3 to 5.

5.4. Transient performance

Apart from the steady-state performance, the transient or dynamic performance of the LAMEE is also very important. The LAMEE should be able to react timely to inlet or control operation condition changes, such as weather changes and initial start-up changes. If the LAMEE does not react quickly enough during transient operational processes, the LAMEE may not transfer enough heat and moisture such that the desired outlet air conditions will not be achieved in a timely manner

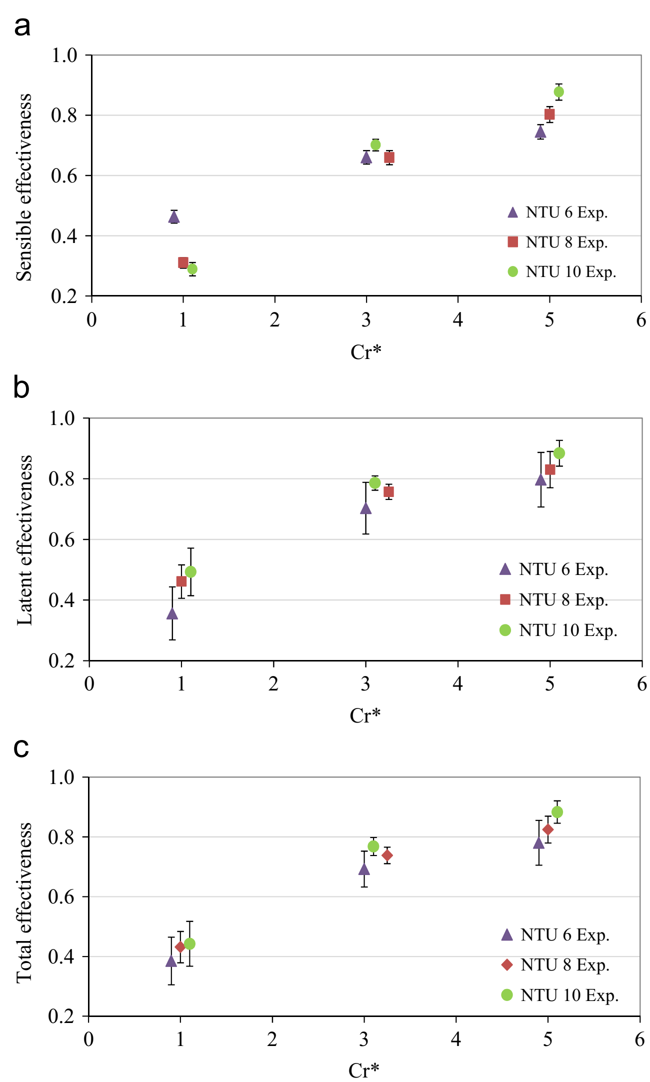


Fig. 14. Steady-state (a) sensible, (b) latent and (c) total effectiveness versus Cr^* for a LAMEE under summer standard test conditions [47].

which will put extra load on the other equipment in the HVAC systems. Although many exchangers have small transient time constants, LAMEEs have time constants that are about 10 times larger

than conventional HVAC heat exchangers. These larger time constants are due to the large thermal capacity of LAMEEs and the coupled heat and moisture transfers transport time delays that occur in LAMEEs. For instance, Erb et al. [29] found that it may take over 5 h to reach steady-state for a RAMEE with two LAMEEs.

Experimental investigations about the transient performance of LAMEEs were performed. It was found that the effectiveness increased during transient period and finally they reached a steady-state value within the uncertainty limits of the numerical results, as shown in Fig. 15 [47]. An exponential correlation with two time constants was fitted to the measured data. For the LAMEE investigated at selected operating conditions, the first time constant was 1–4 min and it was related to the desiccant transport time in the LAMEE while the second time constant was 5–24 min which was related to the thermal mass capacity of the LAMEE. The time constant values increased as Cr* decreased or NTU increased. The LAMEE responded faster at higher air and desiccant mass flow rates.

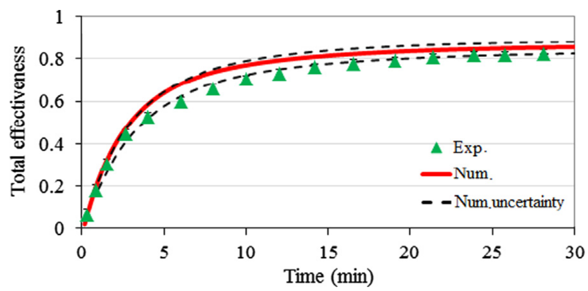


Fig. 15. Transient total effectiveness versus time for a LAMEE under a summer test condition [47].

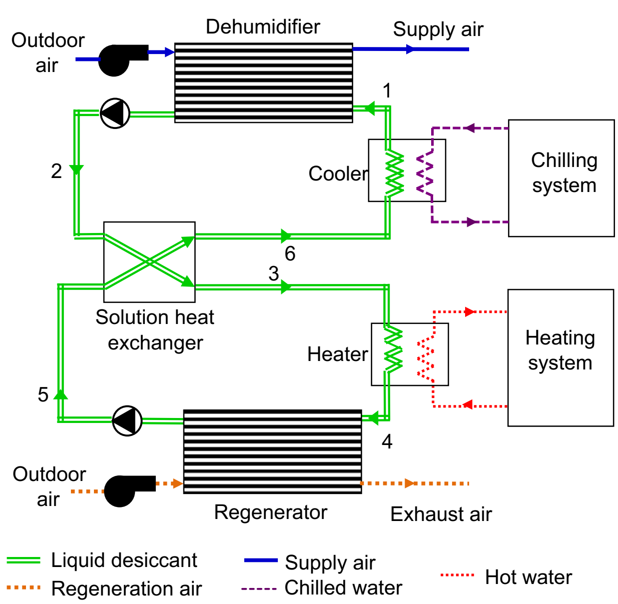


Fig. 16. Schematic of a membrane liquid desiccant air-conditioning system [48].

5.5. Membrane liquid desiccant air-conditioning system

LAMEEs can also be used as active dehumidifier/regenerator in the liquid desiccant air-conditioning (LDAC) systems, as shown in Fig. 16 [48]. It can effectively avoid the desiccant solution air contaminant and downstream drift of liquid desiccant problems in conventional direct-contact liquid desiccant dehumidification systems. Parametric study on steady-state performance of a membrane liquid desiccant dehumidification system has been performed using the TRNSYS energy simulation platform. The impacts of key system parameters, including the solution inlet temperature to the regenerator, solution inlet temperature to the dehumidifier, solution heat exchanger effectiveness, ambient air temperature, ambient air relative humidity, number of heat transfer units, thermal capacity rate ratio, on the system performance were evaluated.

It was found that the LDAC system was suitable for air dehumidification in hot and humid climates, and its overall COP value was between 0.5 and 0.9. The dehumidification capacity (or the outlet supply air humidity) can be effectively controlled by regulating desiccant solution temperatures into regenerator and dehumidifier. The sensible heat ratio lies in a range between 0.3 and 0.5 [48]. Moreover, the system energy efficiency can be significantly improved when solar energy or waste heat is available for desiccant solution regeneration. More research work on the energy performance and control of the LDAC system will be conducted in future.

6. RAMEE performance

6.1. Steady-state performance

A numerical model for RAMEEs was developed and validated by experimental tests using the afore-mentioned test facility. Fig. 17 shows the experimental results and the numerical results for a cross-flow RAMEE at several Cr* values for different NTU values [29]. The experimental data showed that an increase in NTU resulted in an increase in the RAMEE effectiveness, which was also confirmed by the numerical results.

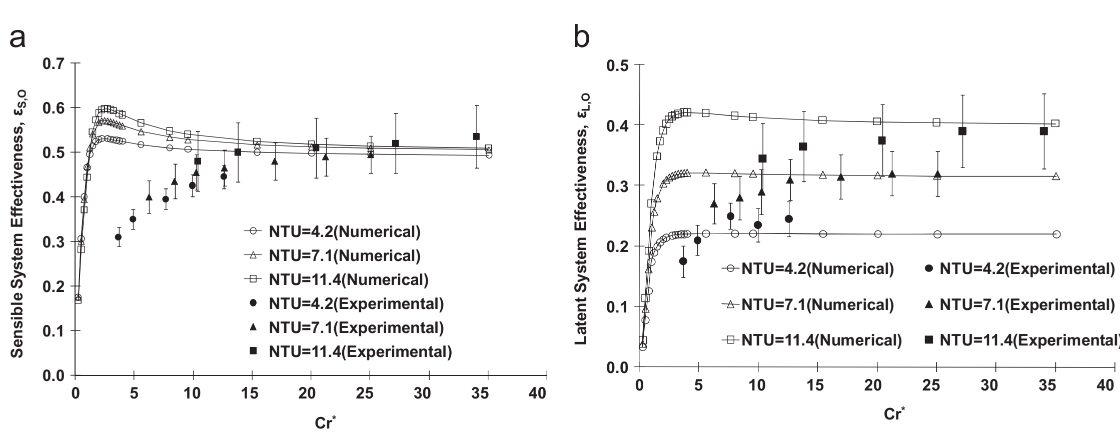


Fig. 17. Numerical and measured (a) sensible, and (b) latent effectiveness versus Cr* at three NTU values under the AHRI summer test conditions [29].

The impacts of NTU and Cr* on the performance of a counter-cross-flow RAMEE were also investigated by numerical simulations. NTU is directly related to the size (i.e. surface area) of an energy exchanger and the fluid mass flow rates. NTU significantly affects the effectiveness of RAMEEs. Fig. 18(a) and (c) shows the impact of NTU on effectiveness of a counter-cross-flow RAMEE system under AHRI summer and winter test conditions [49]. It is observed that the greater the NTU value, the higher the effectiveness, but the slope between effectiveness and NTU decreases as the NTU increases. In practical applications, proper NTU should be considered to give a higher effectiveness and shorter payback period. A design NTU value of up to 10 may be feasible for some applications. The payback period is within five years depending on the climate, RAMEE effectiveness and ventilation rate, etc. [4,50].

The heat capacity ratio (Cr*) characterizes thermal capacity rate of the liquid flow compared to the thermal capacity rate of the air flow in a RAMEE. As shown in Fig. 18(b) and (d), effectiveness increases as Cr* increases at lower Cr* values until the effectiveness reaches a peak value. After the peak value, the effectiveness decreases slightly as the Cr* increases. An optimal Cr* exists and it is dependent on the operating condition (i.e. outdoor air state) and the heat and mass transfer performance of the RAMEE (i.e. U_m). According to the results shown in Fig. 18(b) and (d), the maximum effectiveness of the RAMEE operating at the AHRI summer and winter test conditions occurred approximately at Cr*=3 and Cr*=1.5, respectively.

Hemingson et al. [51] numerically studied the steady-state performance of a RAMEE system for a wide range of outdoor air conditions and found that the effectiveness values were also very dependent on outdoor conditions, as shown in Fig. 19, when the exhaust air condition was constant (i.e. $T_{air,exh}=24\,^{\circ}\mathrm{C}$ and $RH_{air,exh}=50\%$). For some outdoor air conditions near the asymptote (i.e. $\pm\infty$ in the figure), the effectiveness value may exceed 100% or be less than 0%.

6.2. Transient performance

The transient performance of a RAMEE is important during system start-up period or when the outdoor or exhaust air conditions change rapidly. If the RAMEE does not respond quickly, its performance may degrade, and the load on auxiliary heating and cooling equipment may increase. The transient performance of a cross-flow RAMEE system was investigated both numerically and experimentally for summer and winter test conditions. Fig. 20 showed the transient sensible, latent, and total effectiveness results for NTU=11.5 and Cr*=15 at the AHRI summer test conditions [29,38,52].

Fig. 20(a–c) shows that experimental results agree with numerical results for sensible, latent and total effectiveness, when heat losses were considered. If there were no heat losses/gains in the RAMEE, the effectiveness of the supply LAMEE would equal to the effectiveness of the exhaust LAMEE. For the present case, the total effectiveness of the supply LAMEE at the quasi-steady state was 12% higher than that of the exhaust LAMEE. More thermal insulation may reduce the differences between the data and the simulations.

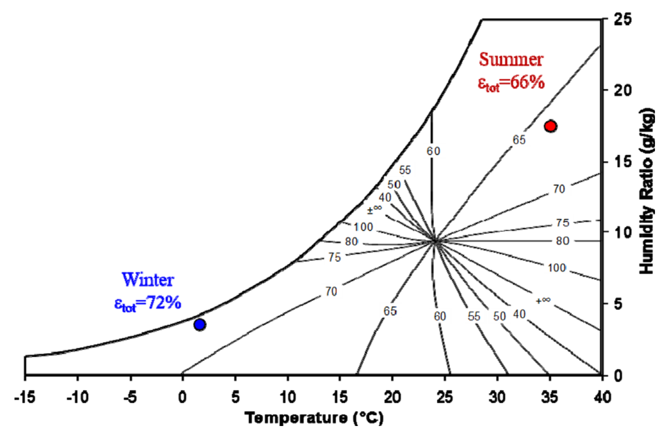


Fig. 19. Total effectiveness of a RAMEE at the two AHRI test conditions for summer and winter and under a wide range of other outdoor air conditions [51].

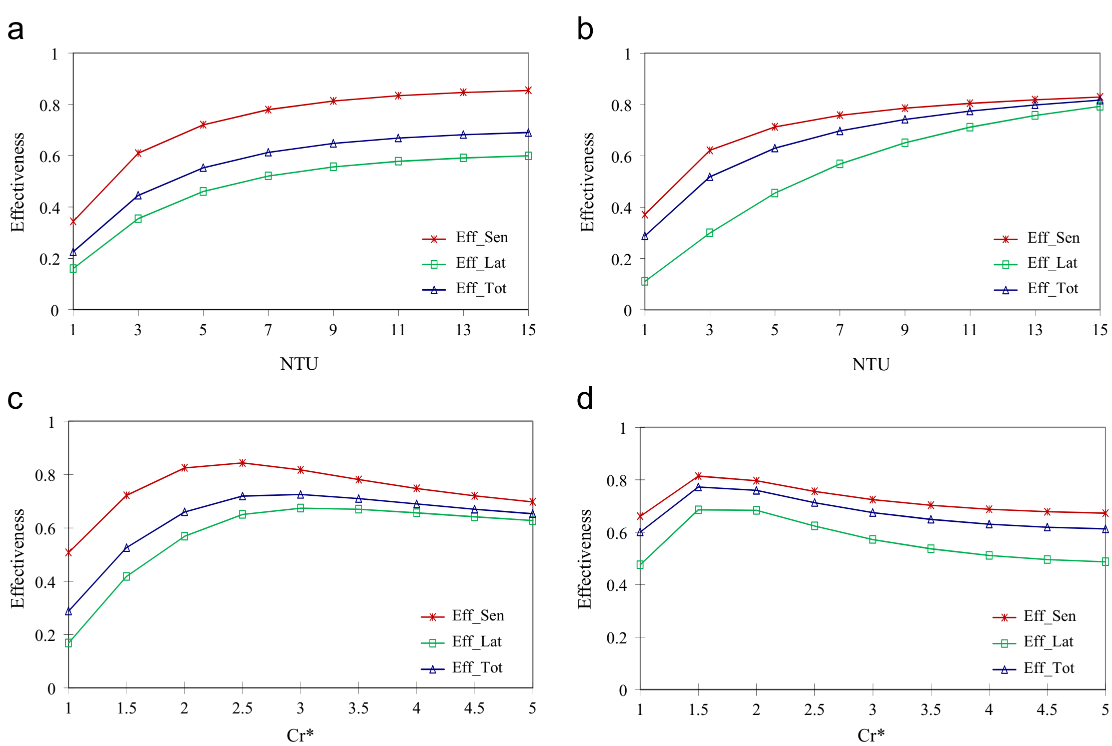


Fig. 18. Effect of NTU and Cr* on RAMEE effectiveness in AHRI summer (a, b) and winter (c, d) conditions [49].

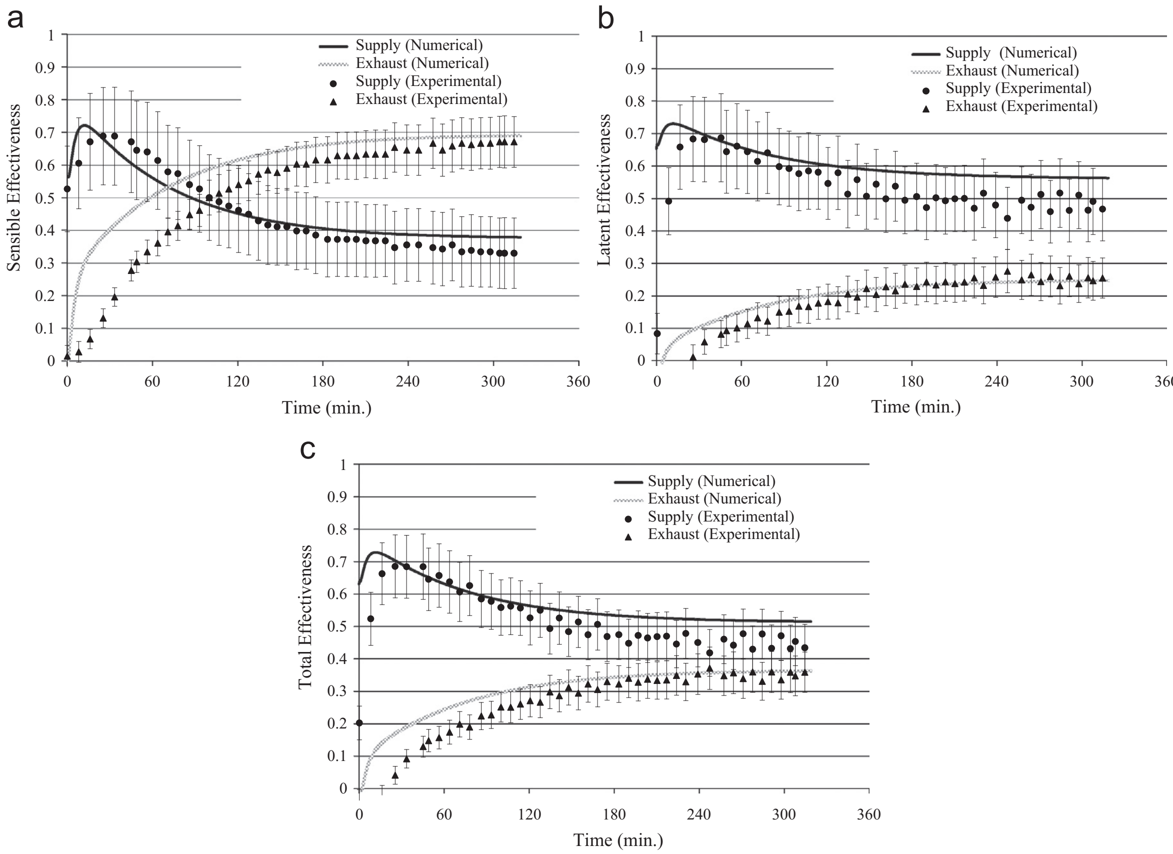


Fig. 20. Transient (a) sensible, (b) latent, and (c) total effectiveness results for a cross-flow RAMEE with NTU = 11.5 and $Cr^* = 15$ during the AHRI summer test condition [29].

The transient response of the RAMEE was quite slow. The quasi-steady state was achieved after around 5 h under these test conditions, which is quite long for practical applications and especially when the weather conditions vary quickly. Consequently, the RAMEE will not be able to response quickly and get adjusted to the new outdoor air conditions. Nevertheless, during the transient period, the effectiveness of the supply LAMEE, which is the most important, was higher than that in the steady-state conditions. This indicated that the RAMEE performance during the transient period was better, therefore longer transient time is beneficial for some conditions and applications. The transient time could be increased by increasing the volume of the desiccant solution in the RAMEE, thus the desiccant solution needs more time to attain the equilibrium temperature and concentration [29].

6.3. *Energy savings potential and payback period*

Using hourly simulations for an office building and a hospital building in four different North American cities, Rasouli et al. [4,50,53] found that a RAMEE provided up to 40%–60% annual heating energy saving and up to 20% annual cooling energy saving in the office and hospital buildings respectively, depending on the climate and RAMEE effectiveness, as shown in Fig. 21. The life-cycle cost analysis showed that the payback period of the ERV was within two years in cold climates and 1–5 years in hot climates, as shown in Table 4. The payback period of ERVs was about two years sooner for the hospital building than in the office building [53]. This difference is caused mostly by the higher ventilation rates required for a hospital. The payback period of RAMEEs was 0 year (instant payback) in some cases, because the use of RAMEEs in HVAC systems can downsize the cooling or heating equipment.

The energy and economic performance of a RAMEE is also impacted by the associated building and HVAC system parameters. An energy and economic analysis of an energy recovery ventilator that can transfer energy between outdoor ventilation air and exhaust air was performed by Rasouli et al. [54]. The results showed that an ERV with 75% sensible and 60% latent effectiveness would reduce the peak heating load by 30%, peak cooling load by 18%, annual heating energy usage by 40% and the annual cooling energy usage by 8%. The cost analysis showed that such an ERV would have a payback period of two years but this payback period was sensitive to its initial cost, recovery effectiveness, energy price, and HVAC equipment initial cost and efficiency as well as ventilation flow rate. A $\pm 25\%$ uncertainty in the seven building input parameters and seven HVAC system input parameters, as shown in Fig. 22, resulted in a maximum 17% and 225% variation in the payback period of the ERV respectively.

6.4. *Control and optimization of RAMEE in HVAC systems*

When the cooling is required during the cool and dry weather, operating of RAMEEs may increase the cooling energy consumption for outdoor ventilation air-conditioning [50,55]. Proper control for the energy recovery system is required to prevent the negative effect and effectively use the free cooling (i.e. economizer when it exists). Whether the RAMEE system should be operated or stopped depends on several factors such as, the indoor and outdoor air conditions and whether the building requires auxiliary heating or cooling energy. Rasouli et al. [4] developed an optimum control strategy for a RAMEE operating with balanced flows in different outdoor conditions, as shown in Fig. 23. If the HVAC system operates during winter (heating mode), the RAMEE's

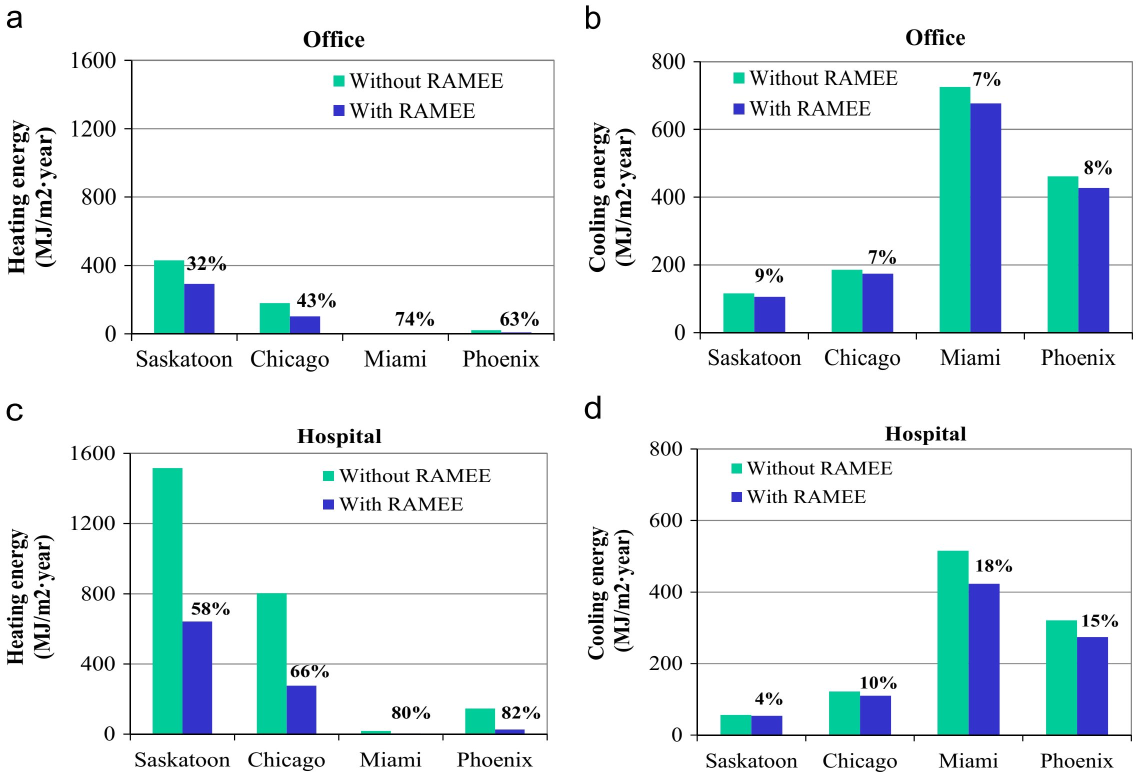


Fig. 21. Energy savings potential of RAMEEs in office and hospital buildings at different cities [53].

Table 4
Payback period (years) of the RAMEEs in different locations and buildings [53].

	Saskatoon	Chicago	Miami	Phoenix
Office	1.8	2	4.8	4
Hospital	0	0	2.5	1.5

sensible effectiveness should be maximized to save heating energy consumption. If the full-load operation at maximum sensible effectiveness heated the outdoor air to a temperature higher than the desired temperature (i.e. part-load operation), then a part of the ventilation air need to be bypassed. If the HVAC system operates during summer (cooling mode), the RAMEE should be turned on only if it is able to decrease the enthalpy of the outdoor ventilation air. The cooling load covered by the cooling coil is directly proportional to the reduction of the outdoor air enthalpy achieved by the RAMEE. If the enthalpy of the outdoor air is higher than the indoor air, the RAMEE should be operated at the maximum total effectiveness. In the cool summer season, if the internal loads (e.g. equipment, lighting, people, etc.) and solar load are high and require the operation of the cooling unit to keep the indoor air at the design conditions, the RAMEE should be switched off to avoid any pre-heating of the cool outdoor air, and an economizer can be used to take more outdoor air to cool the building.

According to previous research results, as shown in Fig. 18, it can be found that the effectiveness of a RAMEE increases firstly at lower Cr* values until it reaches a peak value, after the peak value the effectiveness decreases as the Cr* increases. The optimal Cr* is dependent on the operating condition (i.e. outdoor air state) and the heat and mass transfer performance in the RAMEE. Some studies on the optimal operating Cr* (or coupling solution flow rate) to get the highest performance have been conducted [4,49].

Although a numerical model for counter-cross-flow RAMEEs has been developed and it is accurate to predict the system energy performance. However, it is too computationally time consuming to be used for system design and is not practical for performance optimization for applications. Akbari et al. [25,56] developed neural network (NN) models to predict the steady-state and transient performance of a RAMEE. These NN models were computationally fast and easy to use for system design and optimization. Based on these neural network models, Rasouli et al. [4] developed a TRNSYS simulation program for the prediction of the hourly optimal Cr* at which the RAMEE system operated under the peak performance, as show in Fig. 24. In addition, Ge et al. [49] presented an analytical model for the counter-cross-flow flat-plate LAMEEs based on Zhang's analytical solution for a counter-flow tube-and-shell liquid-to-air contactor [57]. This analytical model can also be used to optimize the Cr* value to get the best performance of RAMEEs. It was found that the optimal Cr* varied from hour to hour as the outdoor conditions changed. Fig. 25 shows the hourly values of optimal Cr* for a RAMEE during one year in Chicago, Illinois. It can be found that the optimal Cr* is higher in summer than in winter. In summer season, the average Cr* is close to 2.71 to operate for peak performance, while in cold season the average Cr* is around 1.76. Overall, the optimal average Cr* is 1.84 for the whole year to achieve maximum energy recovery rate.

In reality, the exhaust air flow rate may be different from the outdoor ventilation air rate due to the building type (i.e. office or hospital) and actual pressure relationship between indoor and outdoor. A research about the energy performance evaluation for RAMEEs under unbalanced air flow conditions has been performed [49]. Fig. 26 shows the total effectiveness of a RAMEE under unbalanced air flow. It can be found that the total effectiveness of the RAMEE increases from 71% to 82% as the exhaust air flow rate ratio (M_{exh}/M_{sup}) increases from 1 to 1.4; while the total effectiveness decreases from 71% to 49% as the exhaust air rate is

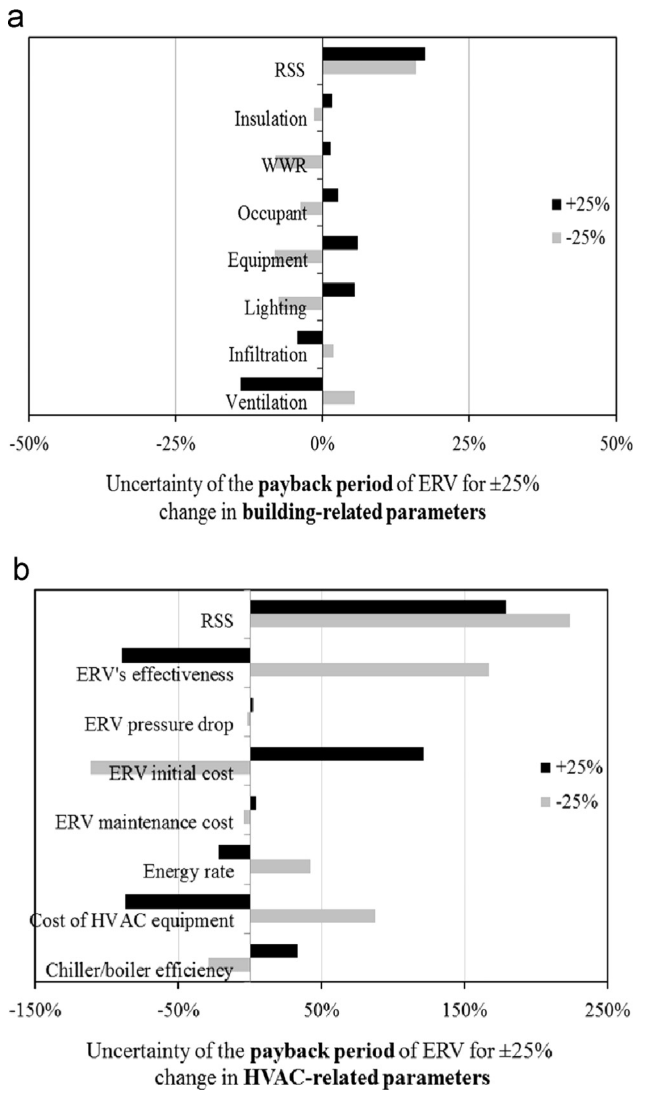


Fig. 22. Uncertainty of ERV's payback period to (a) building-related parameters and (b) HVAC-related parameters [54].

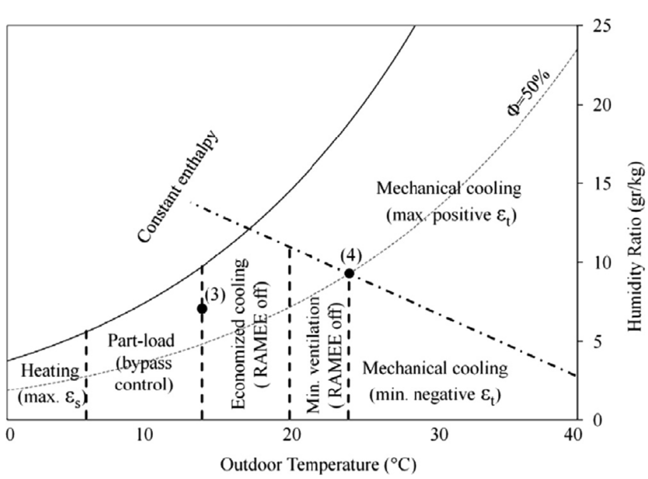


Fig. 23. Operating condition of a RAMEE system in different outdoor conditions [4].

reduced to 60% of the ventilation rate. Therefore, in practical applications, the HVAC designers and building operators should maximize the exhaust air flow in the RAMEE to obtain the greatest

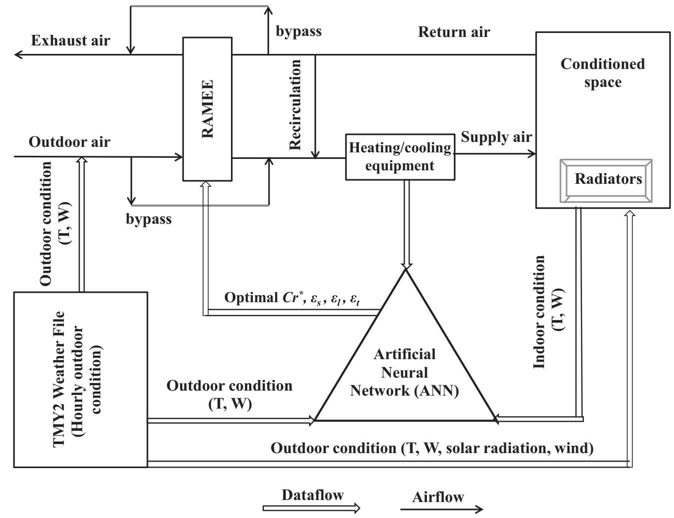


Fig. 24. Schematic of the optimization process for Cr^* in a RAMEE based on ANN models [4].

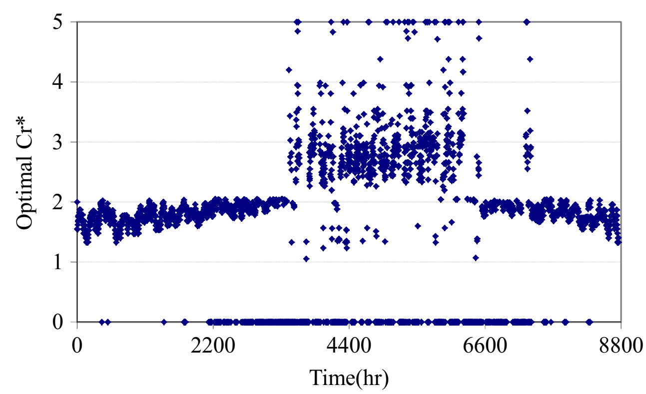


Fig. 25. Hourly optimal Cr^* values for a RAMEE in Chicago in a whole year [49].

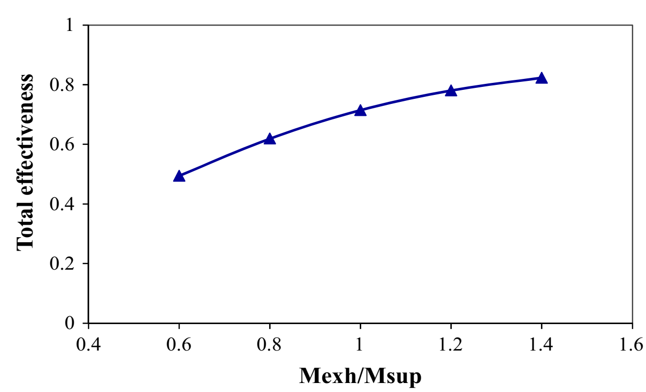


Fig. 26. Total effectiveness of a RAMEE under different exhaust air flow rates [49].

reduction in ventilation air-conditioning costs; however, building envelop considerations may result in changes to this finding.

7. Conclusions

This paper reviews the research done in the Thermal Science Laboratory at the University of Saskatchewan in the past 10 years. A new liquid-to-air membrane energy exchanger (LAMEE) was developed, and progress has been made on the research and applications of LAMEEs in building HVAC systems. The detailed topics studied include: properties and selection of membranes,

properties and selection of desiccant solutions, LAMEE design, steady-state and transient performance of single LAMEEs, energy and economic performance of run-around membrane energy exchanger (RAMEE) systems (typically consisting of two LAMEEs) for passive energy recovery in building HVAC systems and performance of liquid desiccant air-conditioning (LDAC) systems using LAMEEs as active dehumidifiers and regenerators. The proposed RAMEE system can achieve up to 60% annual heating energy saving and up to 20% annual cooling energy saving in the building HVAC systems, depending on the climate, building type and RAMEE effectiveness, etc. The payback period of the RAMEE system was within two years in cold climates and within five years in hot and humid climates. Related control and optimization methods were also developed for practical applications. In addition, the proposed LDAC system was energy-efficient for air dehumidification in humid and hot climates, with a COP between 0.5 and 0.9. The sensible heat ratio was lower in the range of 0.3–0.5 and liquid desiccant carryover problem can be avoided. More research work on the energy performance and control of the LDAC system will be conducted in future.

Acknowledgments

This research was financially supported by the Natural Sciences and Engineering Research Council of Canada (NSERC) and Venmar CES, Inc., Saskatoon, SK, Canada. The authors are also grateful to the researchers and students involved in this project and related projects at the University of Saskatchewan over the past decade. They are: Wei Shang, Stephen Olutimayin, Yiheng Wang, Haisheng Fan, Oyetope Abe, Olalekan Osanytintola, Melanie Fauchoux, Michael Larson, Conrad Iskra, Chris Richards, Prabal Talukdar, Meng Li, Mehran Seyed-Ahmadi, Chris James, Alireza Vali, Khizir Mahmud, Blake Erb, Mohammad Afshin, Howard Hemingson, Mohammad Rasouli, Philip LePoudre, David Beriault, David Pyra, Gazi Mahmood, Soheil Akbari, Ramin Namvar, Hiren Patel, Davood Ghadiri, Radia Eldeeb, Ashkan Oghabi, Ahmed Abdel-Salam and Mohammad Rafati.

References

[1] BP Statistic Review of World Energy June 2012. bp.com/statisticalreview.
[2] Lior N. Sustainable energy development (May 2011) with some game-changers. Energy 2012;40(1):3–18.
[3] Perez-Lombard L, Ortiz J, Pout C. A review on buildings energy consumption information. Energy and Buildings 2008;40(3):394–8.
[4] Rasouli M, Akbari S, Hemingson H, Besant RW, Simonson CJ. Application of a run-around membrane energy exchanger in an office building HVAC system. ASHRAE Transactions 2011;117(2):686–703.
[5] Simonson CJ, Shang W, Besant RW. Part-load performance of energy wheels. Part I. Wheel speed control. ASHRAE Transactions 2000;106(1):286–300.
[6] Besant RW, Simonson CJ. Air-to-air energy recovery. ASHRAE Journal 2003; 45(4):42–52.
[7] Jeong JW, Mumma SA. Practical thermal performance correlations for molecular sieve and silica gel loaded enthalpy wheels. Applied Thermal Engineering 2005;25(5–6):719–40.
[8] Zhang LZ, Niu JL. Energy requirements for conditioning fresh air and the long-term savings with a membrane-based energy recovery ventilator in Hong Kong. Energy 2001;26(2):119–35.
[9] Liang CH, Zhang LZ, Pei LX. Performance analysis of a direct expansion air dehumidification system combined with membrane-based total heat recovery. Energy 2010;35(9):3891–901.
[10] Xiao F, Ge GM, Niu XF. Control performance of a dedicated outdoor air system adopting liquid desiccant dehumidification. Applied Energy 2011;88(1):143–9.
[11] ASHRAE. HVAC systems and equipment handbook.Air-to-air energy recovery. Atlanta: ASHRAE; 2008 [chapter 44].
[12] Mei L, Dai YJ. A technical review on use of liquid-desiccant dehumidification for air-conditioning application. Renewable and Sustainable Energy Reviews 2008;12(3):662–89.
[13] Daou K, Wang RZ, Xia ZZ. Desiccant cooling air conditioning: a review. Renewable and Sustainable Energy Reviews 2006;10(2):55–77.
[14] Fumo N, Goswami DY. Study of an aqueous lithium chloride desiccant system: air dehumidification and desiccant regeneration. Solar Energy 2002;72(4): 351–61.
[15] Liu XH, Jiang Y, Qu KY. Heat and mass transfer model of cross flow liquid desiccant air dehumidifier/regenerator. Energy Conversion and Management 2007;48(2):546–54.
[16] Dai YJ, Zhang HF. Numerical simulation and theoretical analysis of heat and mass transfer in a cross flow liquid desiccant air dehumidifier packed with honeycomb paper. Energy Conversion and Management 2004;45(9–10): 1343–56.
[17] Yin YG, Zhang XS, Wang G, Luo L. Experimental study on a new internally cooled/heated dehumidifier/regenerator of liquid desiccant system. International Journal of Refrigeration 2008;31(5):857–66.
[18] Liu XH, Chang XM, Xia JJ, Jiang Y. Performance analysis on the internally cooled dehumidifier using liquid desiccant. Building and Environment 2009;44(2): 299–308.
[19] Kinsara AA, Elsayed MM, Al-Rabghi OM. Proposed energy-efficient air conditioning system using liquid desiccant. Applied Thermal Engineering 1996;16 (10):791–806.
[20] Dai YJ, Wang RZ, Zhang HF, Yu JD. Use of liquid desiccant cooling to improve the performance of vapor compression air conditioning. Applied Thermal Engineering 2001;21(12):1185–202.
[21] Liu XH, Geng KC, Lin BR, Jiang Y. Combined cogeneration and liquid-desiccant system applied in a demonstration building. Energy and Buildings 2004;36(9): 945–53.
[22] Kinsara AA, Al-Rabghi OM, Elsayed MM. Parametric study of an energy efficient air conditioning system using liquid desiccant. Applied Thermal Engineering 1997;18(5):327–35.
[23] Tu M, Ren CQ, Zhang LA, Shao JW. Simulation and analysis of a novel liquid desiccant air-conditioning system. Applied Thermal Engineering 2009;29(11–12): 2417–25.
[24] Xiong ZQ, Dai YJ, Wang RZ. Development of a novel two-stage liquid desiccant dehumidification system assisted by $CaCl_2$ solution using exergy analysis method. Applied Energy 2010;87(5):1495–504.
[25] Akbari S, Hemingson HB, Beriault D, Simonson CJ, Besant RW. Application of neural networks to predict the steady state performance of a run-around membrane energy exchanger. International Journal of Heat and Mass Transfer 2012;55(5–6):1628–41.
[26] Mahmud K, Mahmood GI, Simonson CJ, Besant RW. Performance testing of a counter-cross-flow run-around membrane energy exchanger (RAMEE) system for HVAC applications. Energy and Buildings 2010;42(7):1139–47.
[27] Simonson CJ, Besant RW. Energy wheel effectiveness: part I—development of dimensionless groups. International Journal of Heat and Mass Transfer 1999;42(12):2161–70.
[28] ASHARE. ANSI/ASHRAE standard 84 method of testing air-to-air heat exchangers. Atlanta: ASHRAE; 2008.
[29] Erb B, Ahmadi MS, Simonson CJ, Besent RW. Experimental measurements of a run-around membrane energy exchanger with comparison to a numerical model. ASHRAE Transactions 2009;115(2):689–705.
[30] Mahmud K. Design and performance testing of counter-cross-flow run-around membrane energy exchanger system [Master's thesis] Saskatoon, Saskatchewan, Canada: University of Saskatchewan; 2009.
[31] AHRI. ANSI/ARI standard 106, standard for rating air-to-air exchangers for energy recovery ventilation equipment. Arlington, VA: Air-Conditioning & Refrigeration Institute; 2005.
[32] ISO. ISO Standard 5167.1, Measurement of fluid flow by means of pressure differential devices. Geneva, Switzerland: International Organization for Standardization; 1991.
[33] Larson MD, Simonson CJ, Besant RW, Gibson PW. The elastic and moisture transfer properties of polyethylene and polypropylene membranes for use in liquid-to-air energy exchangers. Journal of Membrane Science 2007;302(1–2): 136–49.
[34] Beriault DA. Run-around membrane energy exchanger prototype 4 design and laboratory testing [Master's thesis] Saskatoon, Saskatchewan, Canada: University of Saskatchewan; 2011.
[35] Hemingson HB, Simonson CJ, Besant RW. Effects of non-uniform channels on the performance of a run-around membrane energy exchanger (RAMEE). In: Proceedings of 12th international conference on air distribution in rooms (ROOMVENT 2011). Trondheim, Norway; June 19–22 2011.
[36] Larson MD, Besant RW, Simonson CJ. The effect of membrane deflections on flow rate in cross flow air-to-air exchangers. HVAC&R Research 2008;14(2): 275–88.
[37] Erb B. Run-around membrane energy exchanger performance and operational control strategies [Master's thesis] Saskatoon, Saskatchewan, Canada: University of Saskatchewan; 2009.
[38] Seyed-ahmadi M, Erb B, Simonson CJ, Besant RW. Transient behavior of run-around heat and moisture exchanger system, Part I: model formulation and verification. International Journal of Heat and Mass Transfer 2009;52(25–26): 6000–11.
[39] Afshin M, Simonson CJ, Besant RW. Crystallization limits of LiCl–water and $MgCl_2$–water salt solutions as operating liquid desiccant in the RAMEE system. ASHRAE Transactions 2010;116(2):494–506.
[40] Afshin M. Selection of the liquid desiccant in a run-around membrane energy exchanger. [Master's thesis] Saskatoon, Saskatchewan, Canada: University of Saskatchewan; 2010.

[41] Vali A. Modeling a run-around heat and moisture exchanger system using two counter/cross flow exchangers [Master's thesis] Saskatoon, Saskatchewan, Canada: University of Saskatchewan; 2009.
[42] ASHRAE. Energy standard for buildings except for low-rise residential buildings. ANSI/ASHRAE Standard 90.1-2007. ASHRAE: Atlanta; 2007.
[43] Fan HS. Modeling a run-around heat and moisture recovery system [Master's thesis] Saskatoon, Saskatchewan, Canada: University of Saskatchewan; 2005.
[44] LePoudre P, Simonson CJ, Besant RW. Channel flow with sinusoidal screen insert. In: Proceedings of the 19th annual conference of the CFD society of Canada. Montreal, Quebec; April 28–29 2011.
[45] Fan H, Simonson CJ, Besant RW, Shang W. Run-around heat recovery system using cross-flow flat-plate heat exchangers with aqueous ethylene glycol as the coupling fluid. ASHRAE Transaction 2005;111(1):901–10.
[46] Fan H, Simonson CJ, Besant RW, Shang W. Performance of a run-around system for HVAC heat and moisture transfer applications using cross-flow plate exchangers coupled with aqueous lithium bromide. HVAC&R Research 2006;12(2):313–36.
[47] Namvar R, Pyra D, Ge GM, Simonson CJ, Besant RW. Transient characteristics of a liquid-to-air membrane energy exchanger experimental data with correlations. International Journal of Heat and Mass Transfer 2012;55(23–24): 6682–94.
[48] Abdel-Salam AH, Ge GM, Simonson CJ. Performance analysis of a membrane liquid desiccant air-conditioning system. Energy and Buildings 2013;62:559–69.
[49] Ge GM, Ghadiri Moghaddam D, Namvar R, Simonson CJ, Besant RW. Analytical model based performance evaluation, sizing and coupling flow optimization of liquid desiccant run-around membrane energy exchanger systems. Energy and Buildings 2013;62:248–57.
[50] Rasouli M, Simonson CJ, Besant RW. Applicability and optimum control strategy of energy recovery ventilators in different climatic conditions. Energy and Buildings 2010;42(9):1376–85.
[51] Hemingson HB, Simonson CJ, Besant RW. Steady-state performance of a run-around membrane energy exchanger for a range of outdoor air conditions. International Journal of Heat and Mass Transfer 2011;54(9–10):1814–24.
[52] Seyed-ahmadi M, Erb B, Simonson CJ, Besant RW. Transient behavior of run-around heat and moisture exchanger system, Part II: sensitivity studies for a range of initial conditions. International Journal of Heat and Mass Transfer 2009;52(25–26):6012–20.
[53] Rasouli M. Building energy simulation of a run-around membrane energy exchanger (RAMEE). [Master's thesis] Saskatoon, Saskatchewan, Canada: University of Saskatchewan; 2010.
[54] Rasouli M, Ge GM, Simonson CJ, Besant RW. Uncertainties in energy and economic performance of HVAC systems and energy recovery ventilators due to uncertainties in building HVAC system parameters. Applied Thermal Engineering 2013;50(1):732–42.
[55] Zhou YP, Wu JY, Wang RZ. Performance of energy recovery ventilator with various weathers and temperature set-points. Energy and Buildings 2007; 39(12):1202–10.
[56] Akbari S, Simonson CJ, Besant RW. Application of neural networks to predict the transient performance of a run-around membrane energy exchanger for yearly non-stop operation. International Journal of Heat and Mass Transfer 2012;55(21–22):5403–16.
[57] Zhang LZ. An analytical solution to heat and mass transfer in hollow fiber membrane contactors for liquid desiccant air dehumidification. Journal of Heat Transfer 2011;133(9)092001.1–8.